Journal of Marine Science and Application (2025) 24: 210-223
https://doi.org/10.1007/s11804-024-00456-9

RESEARCH ARTICLE

Effects of Split Injection on Combustion, Emissions, and Intermediate Species of Natural Gas High-Pressure Direct Injection Engine

Lijiang Wei[1], Xiuwei Lu[1], Wenqing Huang[1] and Qimin Song[1]

Received: 23 May 2023 / Accepted: 27 March 2024

Abstract

Using natural gas (NG) as the primary fuel helps alleviate the fossil fuel crisis while reducing engine soot and nitrogen oxide (NO_X) emissions. In this paper, the influences of a novel split injection concept on an NG high pressure direct injection (HPDI) engine are examined. Four typical split injection strategies, namely split pre-injection of pilot diesel (PD) and NG, split post-injection of PD and NG, split pre-injection of NG, and split post-injection of PD, were developed to investigate the influences on combustion and emissions. Results revealed that split pre-injection of NG enhanced the atomization of PD, whereas the split post-injection of NG lowered the temperature in the core region of the PD spray, resulting in the deterioration of combustion. The effect of the split injection strategy on indicated thermal efficiency exceeded 7.5%. Split pre-injection was favorable to enhancing thermal efficiency, whereas split post-injection was not. Ignition delay, combustion duration, and premixed combustion time proportion were affected by injection strategies by 3.8%, 50%, and 19.7%, respectively. Split pre-injection increased CH_4 emission in the exhaust. Split post-injection, especially split post-injection of PD and NG, reduced the unburned CH_4 emission by approximately 30%. When the split post-injection ratio was less than 30%, the trade-off between NO_X and soot was interrupted. The distribution range of hydroxyl radicals was expanded by pre-injection, and NO_X was generated in the region where the NG jet hit the wall. This paper provides valuable insights into the optimization of HPDI injection parameters.

Keywords High pressure direct injection; Natural gas; Split injection strategy; Injection ratio; Combustion

1 Introduction

Diesel engines are vastly used in human activities and social production (Wei et al., 2015). Stricter regulations to limit pollutant emissions, the fossil fuel crisis, and the continuous development of alternative fuels have all promoted the development of diesel engines in a more efficient, cleaner direction. Natural gas (NG), with satisfactory combustion performance, lower pollutant emissions, abundant reserves, and low prices, is considered one of the most attractive alternative fuels (Wei and Geng, 2016; Thangaraja and Kannan, 2016). Fuel port injection (FPI) premixed combustion and high-pressure direct-injection (HPDI) diffusion combustion are two ways in which NG is applied in engines (Wei and Geng, 2016; Lu et al., 2020). Lounici et al. (2014) and Gharehghani et al. (2015) performed related research on the combustion and emissions of engines in FPI mode at high, medium, and low loads. Their results revealed that using NG as the main fuel accomplished a synergistic decrease in fuel consumption, nitrogen oxide (NO_X), and soot emissions but increased the emissions of unburned hydrocarbon and carbon monoxide (CO). Wang et al. (2016) investigated the influence of the injection timing of pilot diesel (PD) on the combustion mode of an NG engine in FPI mode. Unlike diesel combustion, advancing PD injection timing leads to a two-stage auto ignition, and pre-injected PD can enhance pollutant emissions at low loads. Guerry et al. (2016) decreased NO_X emissions by advancing the pre-injection timing of PD but at the expense of reduced combustion stability, increased knock tendency, and increased unburned hydrocarbon and CO emissions. The theoretical results obtained by Papagiannakis et al. (2007) using a two-zone phenomenological model disclosed that the appropriate PD injection mass and injection timing are favorable to the enhancement of thermal efficiency

Article Highlights

- Effects of four typical split injection strategies on an NG HPDI engine are examined.
- Combustion and emissions were compared under different split injection strategy.
- Split pre-injection was favorable to enhancing thermal efficiency but increasing CH_4.
- Trade-off between NO_X and soot disappeared at split post-injection ratio below 30%.

✉ Lijiang Wei
ljwei0630@163.com

[1] Merchant Marine College, Shanghai Maritime University, Shanghai 201306, China

and the reduction of CO. Zoldak et al. (2014) performed a more in-depth and detailed investigation by KIVA to investigate the combustion properties and pollutant production of NG engines in FPI mode. Dissimilarities in the mass of the pre-injection PD can influence the distribution of the combustible mixture, the route and phasing of combustion, and the creation of pollutants. Nithyanandan et al. (2017) used optical technology to examine the combustion of an NG engine working at FPI mode and found that pre-injection PD is greatly beneficial in advancing main injection fuel flame propagation and decreasing soot emissions.

NG high-pressure direct injected diffusion combustion theory was first proposed by Professor Philip Hill (Lu et al., 2020). In the HPDI mode, a small amount of PD is injected at the end of the compression stroke, and then NG is directly injected into the cylinder and ignited by PD (McTaggart-Cowan et al., 2004; 2007). The HPDI mode not only compensates for the low intake efficiency of the FPI mode but also obtains outstanding emissions while guaranteeing fuel economy and efficient combustion, especially at medium and low loads (Mas, 2011; Kalam and Masjuki, 2011). Compared with FPI, the injection strategy of HPDI mode is more diverse and complex, entailing not only the corresponding injection rules of PD and NG but also their phase relationship.

To investigate the influence of fuel injection strategy, the research on the effect of fuel injection strategy on HPDI engines has been continuing. Li et al. (2015) thoroughly studied the performance and combustion properties of an NG engine in HPDI mode. Advancing the PD injection timing, reducing the PD injection pulse width, increasing the PD injection pressure, and shortening the injection interval between PD and NG can reduce fuel consumption. Zoldak et al. (2015) examined the influences of the PD and NG injection strategies on an NG-HPDI engine. They revealed that the multiple injections of PD and NG can remarkably enhance engine performance. Similar to the research conducted by Wang et al. (2016) on an NG engine with FPI mode, Zhang et al. (2015) performed a more targeted qualitative analysis of the fuel consumption rate, in-cylinder pressure (ICP), and NO_X emissions on an NG engine with HPDI mode. They found that when the PD injection timing is advanced, the ICP and NO_X emissions increase, but the fuel consumption rate decreases. Kheirkhah (2015) established a computational fluid dynamic (CFD) model of an NG engine functioning at HPDI mode based on the OpenFOAM program. The results revealed that the minor premixed combustion by postponing the injection timing of PD can suppress particulate matter production. Papagiannakis et al. (2017) integrated experiments and CFD to examine the effect of PD injection timing and NG substitution ratio on the performance and emissions of a single-cylinder NG engine in HPDI mode under different loads. The maximum ICP and CO emissions are positively correlated with the NG substitution ratio and inversely proportional to NO_X and soot emissions. Increasing the injection advance angle of PD can enhance CO and soot emissions. Liu et al. (2019) performed a correlation analysis of injection strategies on a marine two-stroke NG engine working in HPDI mode. Modifying the PD and NG injection timings together is termed absolute injection timing, and changing one of them individually is called relative injection timing. They found that the influence of absolute injection timing on combustion characteristics and emissions is similar to that of diesel engines, whereas the influence of relative injection timing is extremely difficult. Lu et al. (2022) conducted a simulation study of the effect of injection overlap between PD and NG on NO_X and soot emissions of an NG engine in HPDI mode. When the injection overlap is fixed at a 2° crank angle (CA), soot and NO_X emissions can be optimized by retaining the start of injection (SOI) of NG and postponing the end of injection (EOI) of PD.

According to the above literature review, many studies have investigated the influences of individual injection parameters on combustion and emissions in HPDI mode, but the effects of multiple injections and their mechanism have rarely been discussed. Whether multiple injections in HPDI mode achieve the same large benefits for in-cylinder combustion and emissions as in FPI mode (Nithyanandan et al., 2017) remains unknown and needs to be discovered. Moreover, ambiguities remain in understanding the interaction mechanisms between PD and NG, especially under different in-cylinder thermodynamic states. In addition, studies on the connection between the evolution of key combustion intermediates, the in-cylinder combustion, and the generation of major pollutants are few. In this paper, multiple injection strategies of PD and NG are introduced. Single injections of PD and NG are split into multiple injections, which are termed split injections. The influences of simultaneous or separate split injection of PD and NG on combustion and emissions generation are analyzed to obtain insights into the intricate interaction between PD and NG. The kinetic mechanism of the chemical reactions is coupled with CFD to provide a more profound understanding. Moreover, the distribution and evolution of the key combustion intermediates are examined to discover the connection between the key intermediates, in-cylinder combustion, and emission generation. This approach facilitates an in-depth analysis and sheds light on the roles of PD and NG in pre- and post-injection scenarios. The research results offer an important reference for the optimization of HPDI injection parameters.

2 Model validation

2.1 Inflow jet boundary verification

For the NG engine working at HPDI mode, a large

amount of NG was injected into the cylinder in a short duration, and the jet and entrainment characteristics of NG greatly affect the creation of the combustible mixture (Lu et al., 2022; Rahimi et al., 2010). Thus, the accurate description of the NG jet is a crucial part of the study of NG engines in HPDI mode using CFD. In CONVERGE, an "Inflow" boundary was applied on a 0.3 mm diameter circle to simulate high-pressure CH_4 nozzles. CH_4 with a pressure of 4 MPa and temperature of 300 K was injected into a 100 mm×100 mm cylindrical container, and the initial temperature and pressure in the container were 1 MPa and 300 K, respectively. In the solution, the basic grid size was 2 mm, four-level adaptive mesh refinement was performed according to the CH_4 concentration gradient, and two-level fixed embedding was applied in the CH_4 jet direction. The applicability and reliability of the "Inflow" boundary of CH_4 jets were verified by schlieren of 0.4, 1.2, and 2.8 ms after SOI (Wang et al., 2012). Figure 1 shows the comparison results of the experiment and the simulation. The setting of the boundary can capture the spray shape and the development changes of the CH_4 jet.

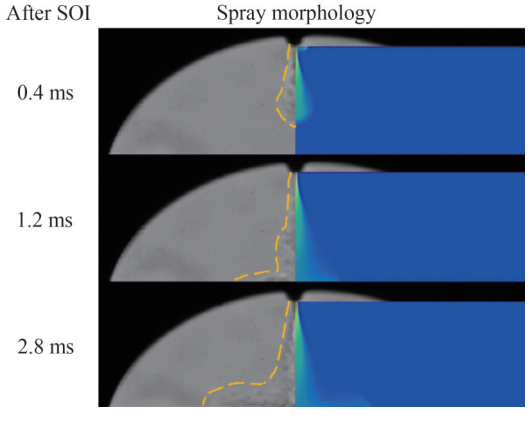

Figure 1 Comparison of CH_4 spray morphology and development: experiment schlieren (left) and simulation (right)

2.2 Engine model validation

The CFD model was established and verified based on the engine parameters and experimental data published by Kheirkhah (2015). The engine parameters are briefly described in Table 1, and the geometric model when the piston is at the top dead center (TDC) is shown in Figure 2. The solution of turbulent motion is the key to determining the accuracy of CFD calculation. The RNG $k-\varepsilon$ model is more appropriate for solving the turbulent motion in the cylinder compared with the standard $k-\varepsilon$ model (Lu et al., 2022). N-heptane was used as a substitute for the physical and chemical properties of PD (Wang et al., 2012). The physical and chemical properties of NG were characterized by 96% CH_4, 2% CO_2, and 2% N_2 (Kheirkhah, 2015). The KH-RT model was used to describe the spray, collision, and breakup of PD (Beale and Reitz, 1999). The jet flow and diffusion of NG were recreated using the previously verified "Inflow" boundary. The SAGE detailed chemical kinetic model was used to solve the chemical reaction of the combustion (Li et al., 2021; 2019), and the solution was coupled with the combustion mechanism developed by Rahimi et al. (2010). The combustion mechanism contained 76 species and 464 reactions, which can accurately solve the NG–PD combustion. The Zeldovich mechanism and Hiroyasu soot model were used to forecast the NO_X and soot emissions (Nagle and Strickland-Constable, 1962; Hiroyasu and Kadota, 1976). The basic grid size of 2 mm was used in the solution. Two-level adaptive mesh refinement was used for in-cylinder temperature (ICT), ICP, and velocity gradient. Moreover, two-level fixed embedding was applied in the injection direction of PD and NG, the upper surface of the piston, and the lower surface of the cylinder. The initial temperature conditions were 553 K for the lower surface of the cylinder head, 523 K for the top surface of the piston, and 433 K for the cylinder wall temperature. The details of the intake air composition and initial conditions for different exhaust gas recirculation (EGR) rates are listed in Table 2.

Table 1 Basic parameter of the engine

Parameters	Value
Bore (mm)	137
Stroke (mm)	169
Compression ratio	17∶1
Displacement (L)	2.5
Engine speed (r/min)	1 500
PD injection mass (mg)	11
SOI_{PD} (°CA)	−17
NG injection mass (mg)	173.7
SOI_{NG} (°CA)	−8

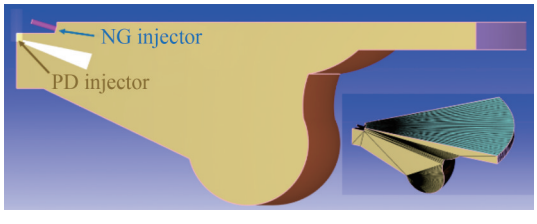

Figure 2 Geometric model of the engine with piston at TDC

Table 2 Initial conditions and intake composition for different EGR rates

Parameter	0% EGR	18% EGR	24% EGR
Pressure (bar)	3.82	4.48	4.5
Temperature (K)	431	441	428
O_2 (%)	0.233	0.205	0.198 3
N_2 (%)	0.767	0.76	0.758 3
CO_2 (%)	0	0.019 4	0.024
H_2O (%)	0	0.015 6	0.019 4

The effectiveness of the model was verified by ICP and HRR at 1 500 r/min, 75% load, and 18% EGR, as well as soot and NO_X emissions at 0%, 18%, and 24% EGR. The coincidence of ICP is encouraging, and the phase of HRR exhibits satisfactory consistency, as shown in Figure 3. Figure 4 compares the experimental and simulated NO_X and soot emissions under diverse EGR rates. The NO_X and soot emissions predicted by the model agree with the experimental values, and the error under all operating conditions is within 5%. The error of HRR is primarily due to the use of n-heptane instead of PD. In addition, the difficulty of decoupling the interaction between PD and NG is the main influence leading to the difference (Kheirkhah, 2015). Generally, the engine model can be used to forecast and assess the in-cylinder combustion and emissions with confidence.

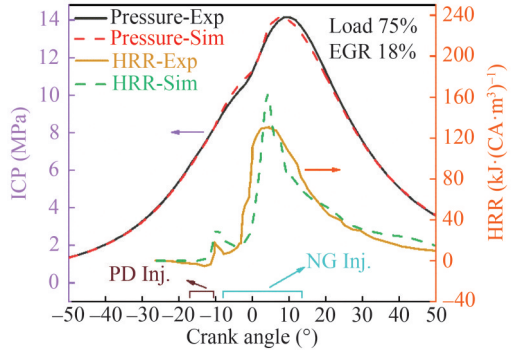

Figure 3 Verification of ICP and HRR at 75% load and 18% EGR

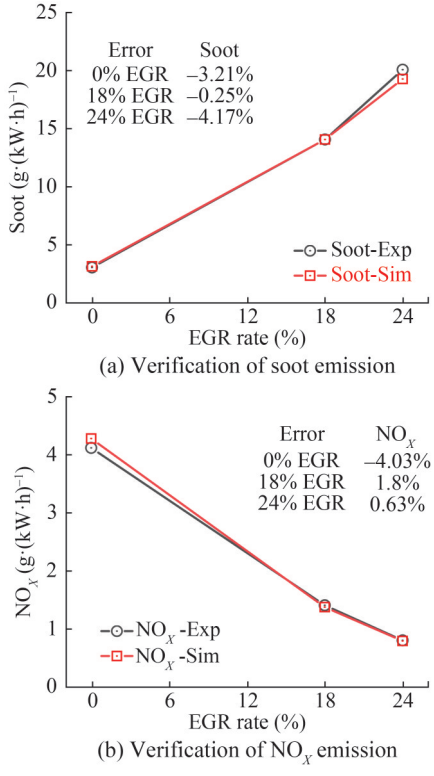

Figure 4 Verification of NO_X and soot emissions under different EGR rates

3 Split injection strategy setting and case selection

3.1 Split injection strategy setting

In this paper, a novel split injection strategy is developed to investigate the interaction mechanism of PD and NG in combustion. Four modes, namely, split pre-injection of PD and NG mode (PRE_{PDNG}), split post-injection of PD and NG mode ($POST_{PDNG}$), split pre-injection of NG mode (PRE_{NG}), and split post-injection of PD mode ($POST_{PD}$), are included in the split injection strategy. For PRE_{PDNG} and $POST_{PDNG}$, the original single injections of PD and NG are divided into two injections. The split pre-injections of PD and NG are organized before the main injections for PRE_{PDNG}, and the split post-injections of PD and NG are placed after the main injections for $POST_{PDNG}$. The split pre-/post-injection ratios of PD are the same as those of NG for PRE_{PDNG} and $POST_{PDNG}$. For example, when 50% of PD is used for split pre-injection in PRE_{PDNG}, the proportion of split pre-injection NG is also 50%. The injection interval between the pre-/post-injection of PD and NG is fixed at 9°CA. For PRE_{NG}, only the original single injection of NG is divided into two injections, and the added one is placed before the main injections of PD and NG. For $POST_{PD}$, only the original single injection of PD is divided into two injections, and the added one is arranged after the main injections of PD and NG. The span between the EOI_{NG} of the split pre-injection and the SOI_{PD} of the main injection or the span between the EOI_{NG} of the main injection and the SOI_{PD} of the split post-injection is defined as the injection interval. The injection intervals of 5°CA, 10°CA, and 15°CA and the split pre-/post-injection ratios of 50%, 30%, and 10% are set for all four modes to explore the effects. The injection durations of PD and NG of all four modes are adjusted closely with the change in injection ratio to ensure consistent injection characteristics. A schematic of the four modes of the split injection strategy is shown in Figure 5. The engine operation condition in all cases is maintained at 75% load, 18% EGR rate, and 1 500 r/min.

3.2 Case selection

The NO_X and soot emissions of all the research cases are shown in Figures 6−9. Figure 6 and Figure 7 present that the split pre-injection strategy has a favorable influence on decreasing soot emissions but a negative effect on NO_X emissions. As the pre-injection ratio increases, soot drops substantially, whereas NO_X increases sharply. The variance in soot emissions between PRE_{NG} and PRE_{PDNG} is slight, whereas that in NO_X emissions is evident. The split pre-injection of PD greatly facilitates the production of NO_X emissions compared with PRE_{NG} primarily because the split pre-injected PD advances the combustion. Overall, under different split pre-injection ratios, with the increase of the

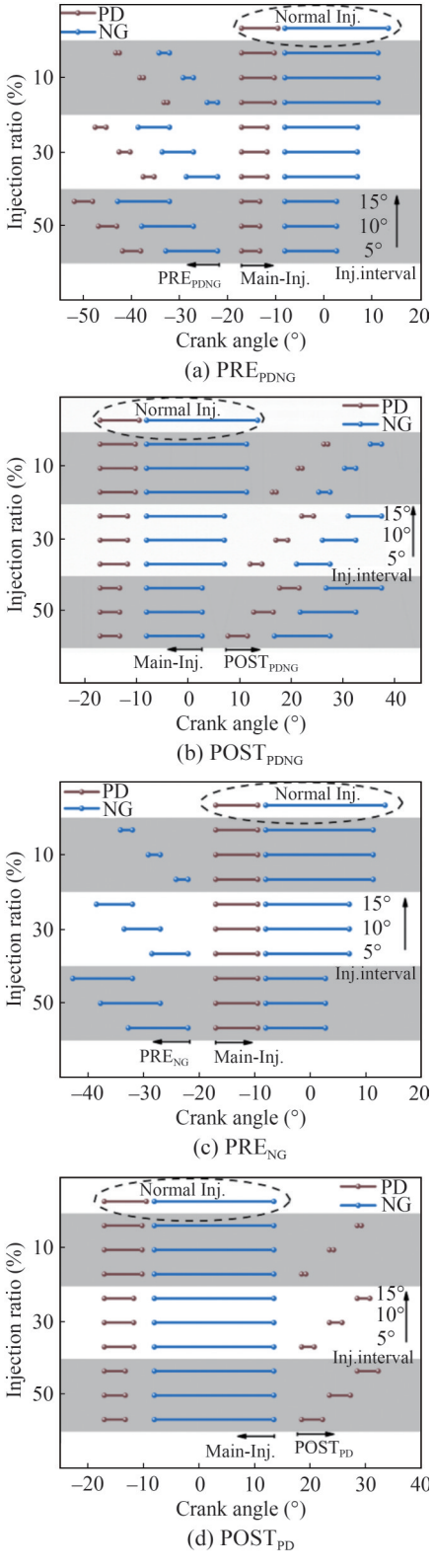

Figure 5 Schematic of injection strategy

injection interval, the NO_X and soot emissions in PRE_{NG} and PRE_{PDNG} modes exhibit diverse variation patterns. This result is primarily associated with the phasing of combustion and the ratio of premixed to diffusion combustion.

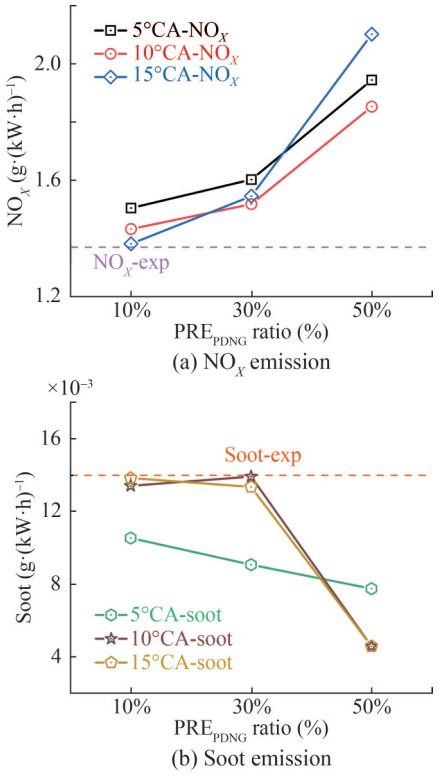

Figure 6 NO_X and soot emissions of PRE_{PDNG}

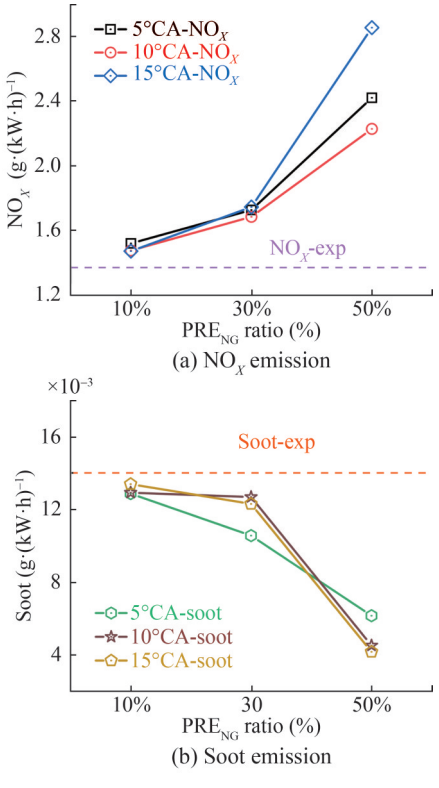

Figure 7 NO_X and soot emissions of PRE_{NG}

Figure 8 and Figure 9 illustrate the NO_X and soot emissions for the split post-injection modes. With the addition

of split post-injections, NO_X and soot emissions demonstrate a completely different trend from that of the split pre-injections. Both split post-injection modes can substantially lessen NO_X emissions, and the reduction of NO_X emissions increases with the increase of the split post-injection ratio. By contrast, soot emissions display different trends in diverse split post-injection modes. In PRE_{PDNG} mode, the soot emissions of different injection intervals exhibit a trend of first decreasing and then increasing with the increase of the split post-injection ratio compared with the experimental single injection. In PRE_{NG} mode, the soot emissions of different injection intervals decrease monotonically with the increase of the split post-injection ratio and are always lower than those of the experimental single injection. It is worth noting that although the $POST_{PDNG}$ mode maintains the trade-off between NO_X and soot emissions, NO_X and soot emissions are immensely improved compared with the experiment when the split post-injection ratio is less than 30%. In the two split post-injection modes of $POST_{PDNG}$ and $POST_{PD}$, the effect of the injection interval on the emissions becomes more apparent with the increase in the post-injection ratio.

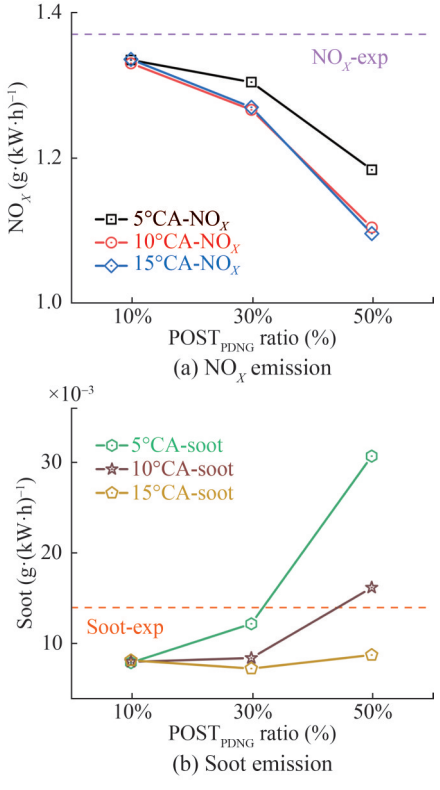

Figure 8 NO_X and soot emissions of $POST_{PDNG}$

The split injection technique has a crucial influence on the NO_X and soot emissions of the NG-HPDI engine. To reveal the roles of PD and NG in the split injection strategy and the interaction mechanism between them, a representative case is chosen from each of the four split injection

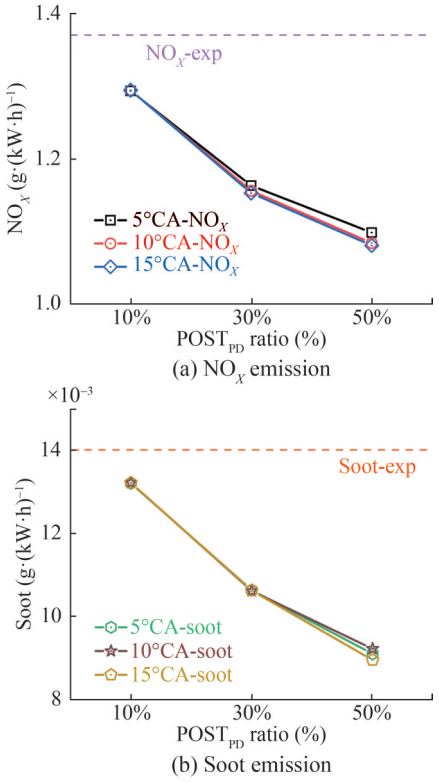

Figure 9 NO_X and soot emissions of $POST_{PD}$

modes in this paper. Through comparative analysis of these cases, the combustion and emission generation processes and important intermediate products are examined and studied. The four cases are listed in Table 3. These cases are chosen based on the lowest NO_X or soot emissions in each split injection mode.

Table 3 Setting of typical cases

Name	Strategy	Ratio (%)	Interval (°CA)
Case 1	PRE_{PDNG}	50	15
Case 2	PRE_{NG}	50	15
Case 3	$POST_{PDNG}$	50	15
Case 4	$POST_{PD}$	50	15
Exp	Experiment	–	–

4 Results and discussion

4.1 Combustion analysis

The combustion of the NG engine in HPDI mode is characterized by not only premixed combustion and diffusion combustion but also particularity (Li et al., 2015; Li et al., 2019; Li et al., 2020; Zheng et al., 2015; Zhang et al., 2022; Macian et al., 2014). According to the working principle, its combustion can be separated into three stages:

ID of PD, premixed combustion of PD and NG, and diffusion combustion of NG. CA10, CA50, and CA90 are the CAs corresponding to 10%, 50%, and 90% of cumulative heat release, respectively. The span between the main injection SOI_{PD} (−17° CA) and CA10 is defined as ID, and the CD is defined as the interval between CA10 and CA90.

The examination of ICT, ICP, and HRR is crucial to investigating the in-cylinder combustion, and the effects of diverse split injection techniques on these parameters are presented in Figure 10. All the split injection strategies display an apparent HRR peak just before TDC. This first HRR peak is formed by the low-temperature oxidation of PD at about 900 K. During this low-temperature oxidation, numerous reactive species are produced and play a decisive role in the subsequent combustion and pollutant generation (Li et al., 2020; Zheng et al., 2015; Zhang et al., 2022; Macian et al., 2014). Figure 10 shows that the split pre-injection does not speed up the low-temperature oxidation but instead lowers the ICT owing to the advance entry of a large amount of fuel. In Case 2, a large amount of NG is pre-injected, which increases the level of in-cylinder turbulent movement and accelerates the formation of the combustible mixture; thus, its ID is shorter, as shown in Figure 11. Case 1 displays a minor increase in ID compared with Case 2 because the heat absorbed by the PD breakup and evaporation further decreases the ICT. For the split post-injection, the two cases exhibit evident two-stage heat release properties. The advantage of the two-stage heat release is that the decrease of the heat release in the first stage reduces the combustion temperature, which can hinder the formation of pollutants, and the increased heat release in the second stage can facilitate the oxidation of pollutants. Compared with Case 3, Case 4 maintains an ICP close to that of Exp, which means Case 4 not only achieves a substantial decrease in pollutant emissions, as shown in Figure 9, but also maintains the working ability.

The combustion phase can more intuitively reflect the influence of the split injection strategy on the combustion. The detailed combustion phasing under diverse strategies is determined, as shown in Figure 11. Constrained by the thermodynamic state in the cylinder, the split pre-injected PD cannot form a self-ignition flame to ignite the NG (Li et al., 2020; Zheng et al., 2015; Zhang et al., 2022; Huang et al., 2019). Thus, the variation in ID under diverse split injection strategies is within 4° CA. These unburned split pre-injected fuels have enough time to form a quasi-homogeneous mixture and then are ignited by the main injection PD and burned rapidly in a premixed combustion manner. The entire combustion is advanced under the split pre-injection strategies (Case 1 and Case 2), CA50 and CA90 are advanced, and the CD is shortened. The reduction of PD injection under the split post-injection strategy prolongs the ID. For Case 4, CA10 is delayed, and the ID is extended by 2.5° CA compared with Exp. This

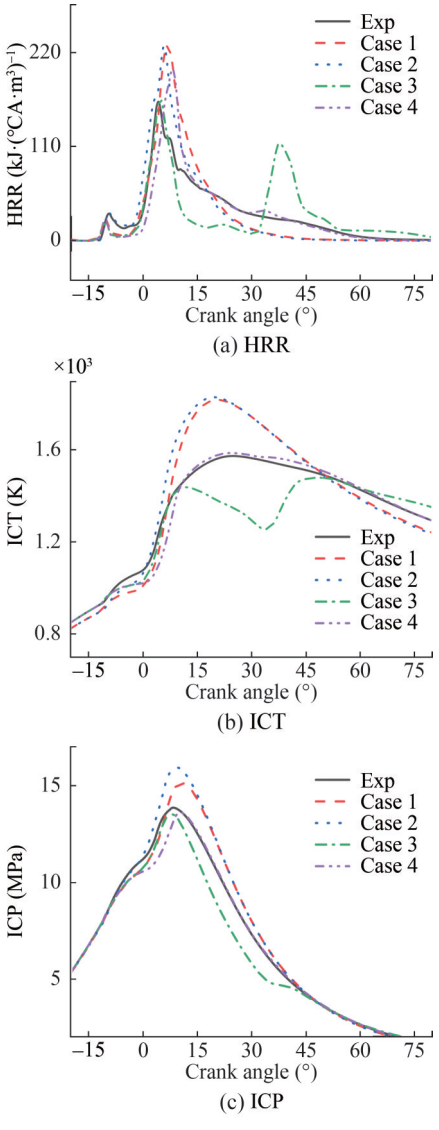

Figure 10 Different ICTs, HRRs, and ICPs in a typical case

condition grants time for the NG to mix, leading to improved premixed combustion, which is primarily why CA50 and CD of Case 4 are still comparable with Exp. However, for Case 3, although the effect of PD reduction on ID is similar to that of Case 4, the split post-injection of the main fuel NG prolongs the entire combustion, leading to a delayed combustion and a substantial increase in the CD. The delayed combustion considerably reduces the ICT of Case 3 in the middle and late stages of combustion. The indicated thermal efficiency under different injection strategies and experimental conditions is presented in Figure 11. The influence of injection strategies on indicated thermal efficiency exceeds 7.5%. Split pre-injection contributes positively to the enhancement of thermal efficiency, whereas split post-injection causes a decrease in thermal efficiency. Split pre-injection without PD inclusion further enhances thermal efficiency, whereas sequential post-injection without NG inclusion helps prevent the decline of thermal efficiency.

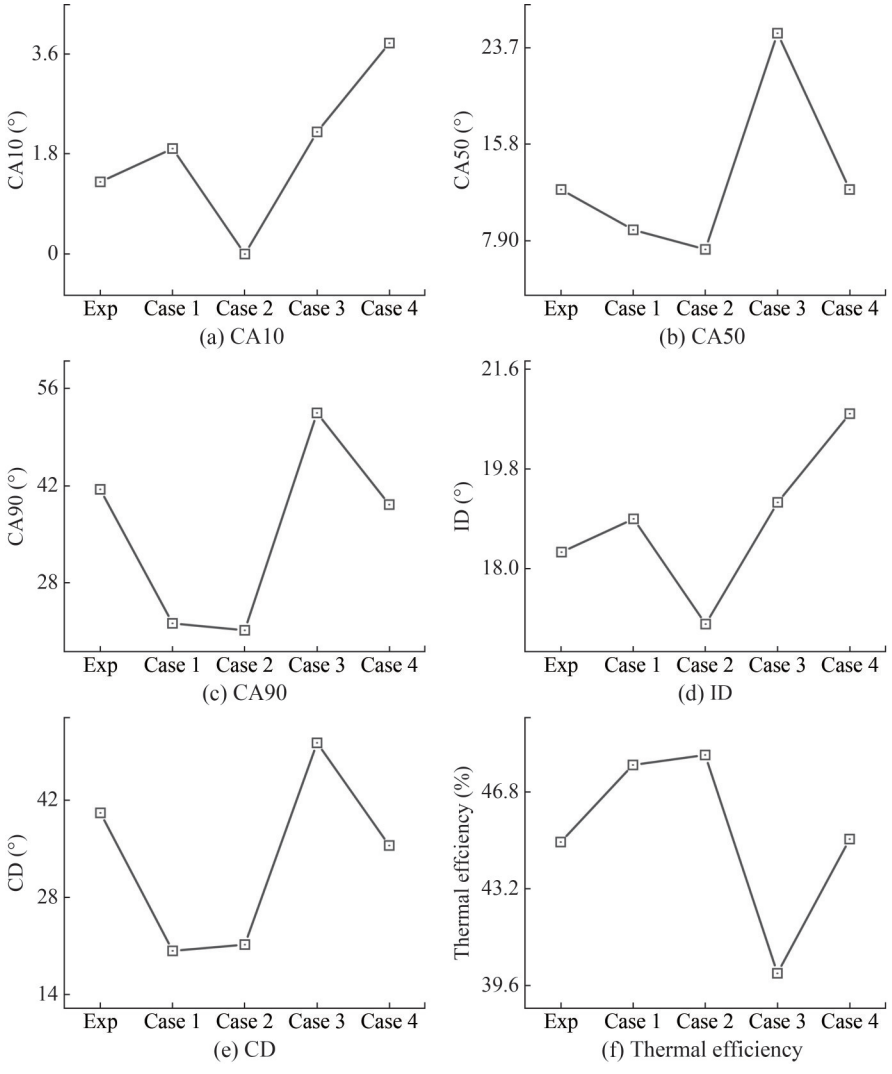

Figure 11 Combustion phase and thermal efficiency of different injection strategies

Elevated temperature is the key to the formation of OH in the region with a suitable equivalence ratio (ER), so the appearance of OH indicates the occurrence of high-temperature premixed combustion (Musculus et al., 2013). In this paper, the position corresponding to the maximum value of OH (M_{OH}) is the demarcation between premixed combustion and diffusion combustion, and the difference between M_{OH} and CA10 is the premixed combustion time. The proportion of premixed combustion time (PPCT) in CD is listed in Table 4. The split pre-injection strategies can increase the PPCT and then increase the ICT and HRR, as shown in Figure 10, which is similar to the combustion model of FPI. The split post-injection of Case 4 slightly increases the PPCT, whereas that of Case 3 has almost no effect on the PPCT. This outcome demonstrates that the effect of split injection on PPCT is connected with the specific strategy. PPCT is inversely proportional to the CD, which means the increase in PPCT increases the speed of combustion. The combustible mixture formed within ID becomes more uniform due to the longer of ID. Although Case 4 and Case 3 have longer IDs, PPCT has a greater variance. This result reveals that the split post-injection of PD or PD and NG results in an entirely dissimilar combustion, and the influence of split post-injection of NG on the combustion is larger. For engines with NG as the main fuel, the mixing state of NG influences the ignition position, ignition timing, and combustion (Zheng et al., 2015; Zhang et al., 2022; Bruneaux, 2008; Mangno et al., 2015).

Table 4 Proportion of premixed combustion

Name	M_{OH} (°CA)	CA10 (°CA)	CD (°CA)	PPCT (%)
Exp	4.1	1.3	40.2	6.96
Case 1	7.6	1.9	20.3	28.07
Case 2	6.1	0	21.2	28.7
Case 3	5.4	2.2	50.3	6.36
Case 4	8.5	3.8	35.5	13.24

4.2 Emission analysis

The process of PD igniting NG not only results in modi-

fications in combustion mode and flame propagation but also influences combustion efficiency and pollutant formation. The change in split injection strategy directly influences the ignition timing, ignition location, and ER distribution near the ignition location (Wang et al., 2016; Guerry et al., 2016; Sankesh and Lappas, 2020; Sankesh et al., 2018). Examining and discussing the changing trends of some key reacting species during the combustion facilitates a more detailed and in-depth understanding of combustion and pollutant formation. Table 5 lists the starting point of PD consumption (C_{PD}) is always ahead of the starting point of CH_2O generation and O_2 consumption (G_{CH_2O} and C_{O_2}), which is not related to the split injection strategy. The split pre-injection of PD (Case 1) makes G_{CH_2O} advance, but combustion does not begin earlier due to low ICT, as shown in Figure 11. The starting point of OH generation (G_{OH}) is earlier than the starting point of NG consumption (C_{NG}), showing that the elevated local temperature generated by PD combustion causes the generation of OH and then ignites NG. These primary combustion products are entirely produced by PD combustion, and the ignition timing of NG is decided by the concentration of these active free radicals and the local temperature in the cylinder. Table 5 shows that the starting points of soot and NO_X generation (G_{soot} and G_{NO_X}) are ahead of C_{NG} and are correlated with C_{O_2} but less related to the split injection strategy.

Table 5 Crank angles for key species generation or consumption

Name	C_{PD} (°CA)	G_{CH_2O} (°CA)	C_{O_2} (°CA)	G_{OH} (°CA)	G_{soot} (°CA)	G_{NO_X} (°CA)	C_{NG} (°CA)
Exp	−14.9	−14.9	−14.1	−11.5	−11.6	−10.3	−3.3
Case 1	−23.8	−23.1	−14.4	−11.8	−11.8	−10.8	−5.1
Case 2	−14.9	−14.8	−14.0	−11.3	−11.5	−10.5	−5.2
Case 3	−15.4	−15.3	−15.1	−12.2	−12.4	−11.3	−5.2
Case 4	−15.4	−15.3	−15.0	−12.2	−12.3	−11.4	−3.2

As the primary component of NG, the greenhouse gas effect of CH_4 is over 25 times that of carbon dioxide (Wei et al., 2016). Therefore, the content of CH_4 in exhaust gases is an important indicator of pollutant emissions in NG-HPDI engines. Figure 12 illustrates the mass fraction of CH_4 when the exhaust valve is open, representing the CH_4 emission. The split pre-injection strategy causes an increase in the CH_4 emission, revealing an increased amount of unburned CH_4. This outcome is ascribed to the early injection of NG diffusing into the cylinder gap, and the lower temperature near the cylinder wall hinders the flame propagation and causes CH_4 to escape, as shown in Figure 14 and Figure 15. Split post-injection, especially when combining the split post-injection of PD and NG, can lessen unburned CH_4 emission by about 30%. During split post-injection, the higher ICT enables the fuel to burn rapidly, preventing NG from diffusing into the clearance area. Thus, the CH_4 emission level in Case 3 is lower, and the split post-injection without NG keeps a level similar to that in the experiment.

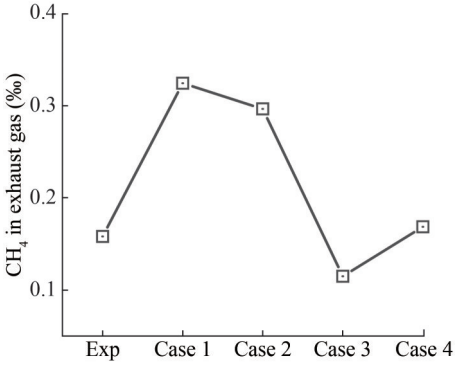

Figure 12 Mass fraction of CH_4 in exhaust gas

4.2.1 Emission analysis of split pre-injection (Case 1 and Case 2)

Figure 13 presents the mass change rates of some key reacting species during the combustion of Exp, Case 1, and Case 2. The mass change rate curves of NG and PD can evidently present the trend of fuel injection and consumption. The value of the mass change rate of O_2 is used as the criterion for determining whether the oxidation reaction occurs and the intensity of the combustion. CH_2O is used to describe the presence of diesel low-temperature decomposition and soot precursors in this region.

CH_2O generation is in accordance with PD consumption, and soot generation begins as CH_2O is consumed. The

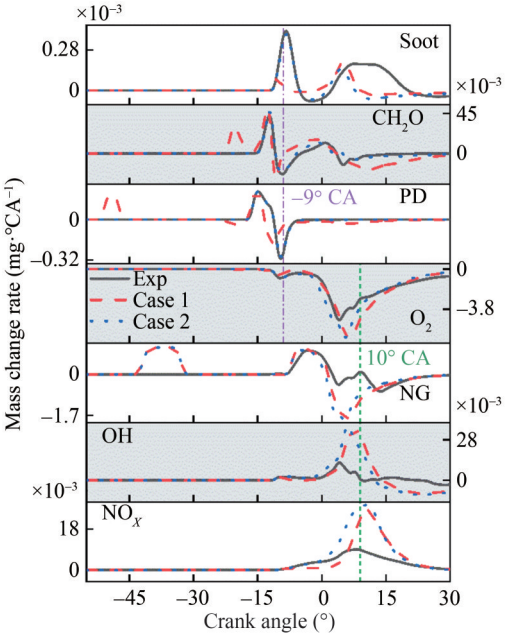

Figure 13 Mass change rate of species (split pre-injection)

variance in the mass change rate of CH_2O is the most direct manifestation of the influence of split pre-injection PD on combustion. CH_2O is one of the main intermediate species created during the low-temperature oxidation of alkane fuel (Bruneaux, 2008; Magno et al., 2015) and can be used as a tracer to suggest the low-temperature oxidation region in the reaction zone (Kosaka et al., 2005). Temperature is a crucial factor in the formation of CH_2O from alkanes in the low-temperature oxidation reaction. Previous studies revealed that 620 K is the lowest temperature observed for CH_2O (Bruneaux, 2008; Kosaka et al., 2005; Magno et al., 2015). Although split pre-injection PD causes G_{CH_2O} to advance, it is constrained by the temperature of the low-temperature oxidation (742 K at −23.8°CA). The ICT and ER distributions and the mass fractions of soot and CH_2O at −9°CA are shown in Figure 14. The interaction between NG and PD is exceptionally strong, and its effects are closely related to the injection technique. The split pre-injected NG rapidly diffuses into the low-temperature cylinder gap area. ER represents the distribution of the combustible mixture formed by PD and NG in the cylinder. Owing to the split injection, the interaction between PD and NG is strengthened, and the PD atomization influence is remarkably enhanced. In Case 1 (PRE_{PDNG}), PD and NG are split pre-injected, and the excellent atomization and mixing influence decreases the rate of soot generation, as shown in Figure 13. In Case 2 and Exp, soot precursors (characterized by CH_2O) are created in the oil-rich region of the PD spray core, and then soot is formed in the high-ICT and ER regions downstream of the spray. Owing to the split pre-injection of PD in Case 1, the distribution of CH_2O in the cylinder is wider, and the area of the high ICT area is smaller. Thus, a small amount of soot is produced in this area. During soot formation, soot precursors are formed in the leading portion of the spray flame after spray ignition. The soot precursors at the periphery of the spray flame are first transformed into soot particles. Young soot particles formed in the central fuel-rich region surrounded by OH regions develop by surface growth and condense during convection to the spray head. At the spray tip, soot particles are pushed to the periphery of the spray through the vortex motion of the head. Finally, the soot particles are transported to the upstream side of the head vortex and are re-entrained in the lean mixture area of the flame, where the OH concentration is higher, and the soot particles are quickly oxidized. The increased rate of OH generation, as shown in Figure 13, and the wider distribution of OH, as shown in Figure 15, contribute to the higher soot oxidation rate at split pre-injection mode, which is also indicated in the rate of soot mass change in Figure 13.

The in-cylinder state at the maximum mass change rate of split pre-injection strategy NO_X (10° CA) is shown in Figure 15. In the Exp, NG is concentrated in the cylinder along the jet direction, and a high-temperature flame front is created at the edge of the jet. On this flame front, OH is distributed in a "banded" shape, forming a "wrapping" influence on the spray. NO_X is produced in the internal region bounded by the flame front and the "banded" OH distribution. The split pre-injection causes the mixture distribution to be wider and more uniform in the cylinder, which is favorable to greater PPCT, as shown in Table 4 and the combustion temperature. The increase of the high-temperature zone with suitable ER (approximately 0.8) facilitates the intensive generation of OH. Regardless of the strategy, NO_X is extremely consistent with high ICT distribution ranges. The difference is that the NO_X of Exp is primarily centered in the periphery of the flame, while the split pre-injection strategy also produces more NO_X in the area where the jet hits the wall.

4.2.2 Emission analysis of split post-injection (Case 3 and Case 4)

Compared with split pre-injection, split post-injection has a more complex influence on combustion. The mass change rates of some key reacting species during the combustion of the split post-injection are presented in Figure 16. Figure 17 presents the distribution of some in-cylinder combustion-

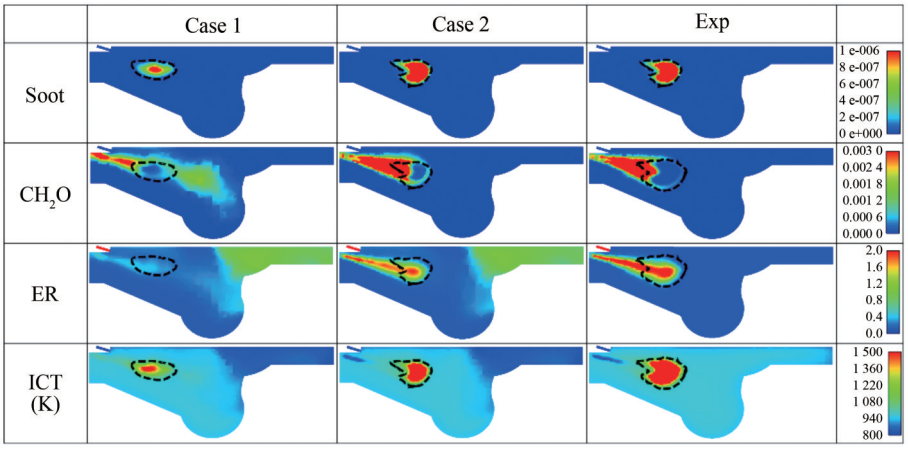

Figure 14 Distribution of ER, ICT, and mass fraction of soot and CH_2O at −9°CA

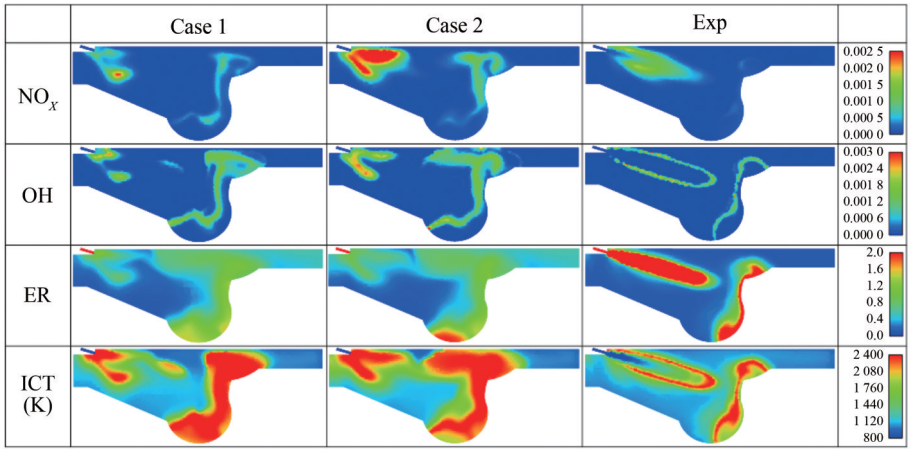

Figure 15 Distribution of ER, ICT, and mass fraction of NO_X and OH at 10°CA

related parameters under the split post-injection strategies at 20°CA and 33°CA. The effect of the injection strategy on combustion is disclosed by comparing Figure 13 and Figure 16. The variation trends of OH and NG under the split post-injection strategy agree with the conclusions acquired under the split pre-injection strategy. The distribution of OH and NO_X is intensely connected with the high-temperature combustion of NG but has slightly correlated with the injection strategy. The difference in O_2 consumption rate between split pre-injection and split post-injection is primarily affected by the combustion rate, which has a corresponding relationship with PPCT. The larger the PPCT, the faster the combustion rate and the larger the peak value of the O_2 mass change rate. The PPCT of Case 4 is between Exp and split pre-injection. The HRR of Case 4 is close to split pre-injection, but its ICT and ICP agree with Exp. This result means Case 4 attains higher HRR while maintaining combustion temperature. The variance in PPCT results in a 44.3% and 60.7% reduction in the maximum mass change rates of OH and NO_X, respectively, in split post-injection compared with split pre-injection.

Figure 17 presents that the soot-generated region coincides with the PD diffusion region. The split pre-injection and split post-injection reveal that PD is the source of soot formed by NG engines in HPDI mode, which agrees with the results achieved by extensive previous studies (Zhang et al., 2015; Papagiannakis et al., 2017; Sankesh and Lappas, 2020). The difference is that the variance in ICT distribution leads to changes in soot generation, and the entrainment outcome of the NG jet causes the soot generation to form pit areas. A low-temperature, oxygen (O_2)-depleted region is created by the split post-injection of a large amount of NG, which generates a large amount of soot in this area. Moreover, the "banded" distribution of OH lessens its effect on soot oxidation, leading to a 22.6% rise in the soot mass change rate compared with split pre-injection. Case 4 has almost no effect on the later combustion, as shown in

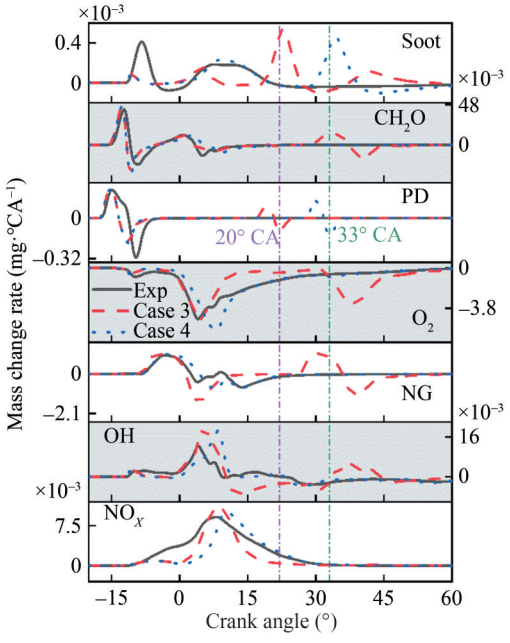

Figure 16 Mass change rate of species (split post-injection)

Figure 11. By contrast, due to the reduction of the main injected PD, the ID becomes longer; thus, Case 4 has a larger PPCT than Case 3 and Exp, as shown in Table 4. The high ICT caused by this prevents the split post-injected PD from undergoing low-temperature oxidation to produce CH_2O, as shown in Figure 17(b). Figure 14, Figure 15, and Figure 17 reveal that the injection timing of NG causes a great discrepancy in the distributions of ER and ICT. The absence of the effect of split post-injected NG is the key to the low soot emission of Case 4. Case 3 cannot decrease NO_X and soot emissions simultaneously as Case 4 because of the large amount of split post-injected NG. The split post-injection NG technique is not a satisfactory option for enhancing in-cylinder combustion and decreasing emission generation.

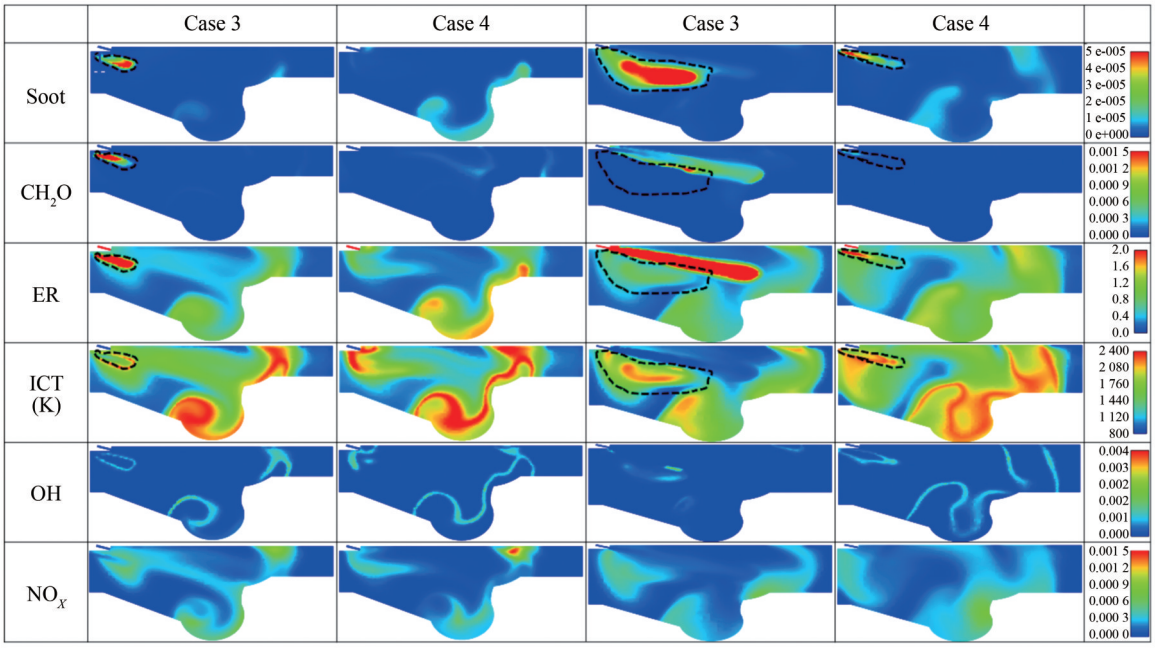

Figure 17 Distribution of soot, CH_2O, NO_X, OH, ER, and ICT

5 Conclusions

The influences of diverse split injection techniques on the combustion performance and emission properties of an NG engine working at HPDI mode are discussed in this paper. The results are examined in detail, and the major concluding remarks are summarized below.

1) The split pre- and post-injection of PD have a limited influence on the HRR curve, whereas the combined split post-injection of PD and NG causes evident two-stage heat release. The split pre-injection of NG increases the combustion speed and improves the indicated thermal efficiency. The effect of different split injection strategies on thermal efficiency exceeds 7.5%.

2) The combustion duration (CD) is shortened, and the PPCT is increased by the split pre-injection. The CD and combustion mode are not influenced by the presence or absence of PD in the split pre-injection. The influences of split post-injection NG on CD and PPCT exceed 30% and 6%, respectively. The ignition delay fluctuates by 3.8%, the CD varies by over 50%, and the PPCT changes by 19.7% under diverse split injection strategies.

3) The split pre-injection of NG remarkably enhances the atomization efficiency of PD but causes a large amount of CH_4 to escape. The split post-injection of NG enters the core area of the PD spray, which decreases the ICT and worsens the combustion.

4) PD is the main source of soot in NG engines in HPDI mode. The mass change rate of soot with the split post-injection strategy is around 21.6% more than that with the split pre-injection strategy, whereas the mass change rate of CH_2O is 12.1% lower. When the post-split-injection ratio is below 30%, the NO_X–soot trade-off is broken.

Nomenclature

CA	Crank angle
CA10	CA corresponding to 10% cumulative heat release
CA50	CA corresponding to 50% cumulative heat release
CA90	CA corresponding to 90% cumulative heat release
CD	Combustion duration
CFD	Computational fluid dynamics
CH_4	Methane
CH_2O	Formaldehyde
CO	Carbon Monoxide
C_{PD}	Starting point of PD consumption
C_{O_2}	Starting point of O_2 consumption
C_{NG}	Starting point of NG consumption
EGR	Exhaust gas recirculation
EOI	End of injection
ER	Equivalence ratio
FPI	Fuel port injection
G_{CH_2O}	Starting point of CH_2O generation
G_{OH}	Starting point of OH generation
G_{soot}	Starting point of soot generation
G_{NO_X}	Starting point of NO_X generation

HPDI	High-pressure direct injection
HRR	Heat release rate
ID	Ignition delay
ICP	In-cylinder pressure
ICT	In-cylinder temperature
NG	Natural gas
NO_X	Nitrogen oxides
OH	Hydroxide
O_2	Oxygen
PD	Pilot diesel
PRE_{NG}	Split pre-injection of NG
PRE_{PDNG}	Split pre-injection of PD and NG
$POST_{PD}$	Split post-injection of PD
$POST_{PDNG}$	Split post-injection of PD and NG
PPCT	Proportion of premixed combustion time
SOI	Start of injection
TDC	Top dead center
M_{OH}	Position corresponding to the maximum value of OH

Funding Supported by the National Natural Science Foundation of China (No. 51909154) and Shanghai Engineering Research Center of Ship Intelligent Maintenance and Energy Efficiency (No. 20DZ2252300).

Competing interest The authors have no competing interests to declare that are relevant to the content of this article.

References

Beale JC, Reitz RD (1999) Modeling spray atomization with the Kelvin-Helmholtz/Rayleigh-Taylor hybrid model. Atomization and Sprays 9(6): 623-650. https://doi.org/10.1615/atomizspr.v9.i6.40

Bruneaux G (2008) Combustion structure of free and wall-impinging diesel jets by simultaneous laser-induced fluorescence of formaldehyde, poly-aromatic hydrocarbons, and hydroxides. International Journal of Engine Research 9(3): 249-265. https://doi.org/10.1243/14680874JER00108

Gharehghani A, Hosseini R, Mirsalim M, Jazayeri SA, Yusaf T (2015) An experimental study on reactivity controlled compression ignition engine fueled with biodiesel/natural gas. Energy 89: 558-567. https://doi.org/10.1016/j.energy.2015.06.014

Guerry ES, Raihan MS, Srinivasan KK, Krishinan SR, Sohail A (2016) Injection timing effects on partially premixed diesel-methane dual fuel low temperature combustion. Applied Energy 162: 99-113. https://doi.org/10.1016/j.apenergy.2015.10.085

Hiroyasu H, Kadota T (1976) Models for combustion and formation of nitric oxide and soot in DI diesel engines. SAE Technical Paper. https://doi.org/10.4271/76012

Huang HZ, Zhu ZJ, Chen YJ, Chen YJ, Lv DL, Zhu JZ, Ouyang TC (2019) Experimental and numerical study of multiple injection effects on combustion and emission characteristics of natural gas-diesel dual-fuel engine. Energy Conversion and Management 183: 84-96. https://doi.org/10.1016/j.enconman.2018.12.110

Kalam MA, Masjuki HH (2011) An experimental investigation of high-performance natural gas engine with direct injection. Energy 36(5): 3563-3571. https://doi.org/10.1016/j.energy.2011.03.066

Kheirkhah P (2015) CFD modeling of injection strategies in a high-pressure direct-injection (HPDI) natural gas engine. Master thesis, University of British Columbia, Vancouver

Kosaka H, Aizawa T, Kamimoto T (2005) Two-dimensional imaging of ignition and soot formation processes in a diesel flame. International Journal of Engine Research 6(1): 21-42. https://doi.org/10.1243/146808705x7347

Li JR, Liu HF, Liu XL, Ye Y, Wang H, Yao MF (2021) Investigation of the combustion kinetics process in a high-pressure direct injection natural gas marine engine. Energy & Fuels 35 (8): 6785-6797. https://doi.org/10.1021/acs.energyfuels.1c00353

Li JR, Liu XL, Liu HF, Ye Y, Wang H, Dong JJ, Liu B, Yao MF (2020) Kinetic study of the ignition process of methane/n-heptane fuel blends under high-pressure direct-injection natural gas engine conditions. Energy & Fuels 34(11): 14796-14813. https://doi.org/10.1021/acs.energyfuels.0c02667

Li JR, Wang JT, Liu T, Dong JJ, Liu B, Wu CH, Ye Y, Wang H, Liu HF (2019) An investigation of the influence of gas injection rate shape on high-pressure direct-injection natural gas marine engines. ENERGIES 12(13): 2571. https://doi.org/10.3390/en12132571

Li MH, Zhang Q, Li GX, Shao SD (2015) Experimental investigation on performance and heat release analysis of a pilot ignited direct injection natural gas engine. Energy 90: 1251-1260. https://doi.org/10.1016/j.energy.2015.06.089

Liu HF, Li JR, Wang JT, Wu CH, Liu B, Dong JJ, Liu T, Ye Y, Wang H, Yao MF (2019) Effects of injection strategies on low-speed marine engines using the dual fuel of high-pressure direct-injection natural gas and diesel. Energy Science & Engineering 7(5): 1994-2010. https://doi.org/10.1002/ese3.406

Lounici MS, Loubar K, Tarabet L, Balistrou M, Niculwscu D, Tazerout M (2014) Towards improvement of natural gas-diesel dual fuel mode: an experimental investigation on performance and exhaust emissions. Energy 64: 200-211. https://doi.org/10.1016/j.energy.2013.10.091

Lu XW, Geng P, Chen YY (2020) NO_X emission reduction technology for marine engine based on tier-III: A review. Journal of Thermal Science 29: 1241-1268. https://doi.org/10.1007/s11630-020-1342-y

Lu XW, Wei LJ, Zhong JJ (2022) Effects of injection overlap and EGR on performance and emissions of natural gas HPDI marine engine. Combustion Science and Technology. https://doi.org/10.1080/00102202.2022.2062568

Macian V, Payri R, Ruiz S, Bardi M, Plazas AH (2014) Experimental study of the relationship between injection rate shape and Diesel ignition using a novel piezo-actuated direct-acting injector. Appl. Energy 118: 100-113. https://doi.org/10.1016/j.apenergy.2013.12.025

Magno A, Mancaruso E, Vaglieco BM (2015) Combustion analysis of dual fuel operation in single cylinder research engine fueled with methane and Diesel. SAE Technical Paper, 2015-24-2461. https://doi.org/10.4271/2015-24-2461

Mas FMA, Yoshiyuki K, Yusuke O, Tomoshi K (2011) Improvement of combustion of CNG engine using CNG direct injection and gas-jet ignition method. SAE Technical Papers, 2011-01-1994. https://doi.org/10.4271/2011-01-1994

McTaggart-Cowan GP, Jones HL, Rogak SN, Munshi, SR, Bushe WK (2007) The effects of high-pressure injection on a compression-ignition, direct injection of natural gas engine. Journal of Engineering for Gas Turbines and Power 129(2): 579-588. https://

doi.org/10.1115/icef2005-1213

McTaggart-Cowan GP, Rogak SH, Hill PG, Bushe WK, Munshi SR (2004) Effect of operating condition on particulate matter and nitrogen oxides emissions from a heavy-duty direct injection natural gas engine using cooled exhaust gas recirculation. International Journal of Engine Research 5(6): 499-511. https://doi.org/10.1177/146808740400500602

Musculus M, Miles PC, Pickett LM (2013) Conceptual models for partially premixed low-temperature diesel combustion. Progress in Energy & Combustion Science 39: 246-283. https://doi.org/10.1016/j.pecs.2012.09.001

Nagle J, Strickland-Constable RF (1962) Oxidation of carbon between 1000–2000 °C. Proceedings of the Fifth Conference on Carbon. 154-164, Pogama. https://doi.org/10.1016/B978-0-08-009707-7.50026-1

Nithyanandan K, Gao Y, Wu H, Lee CF, Liu FS, Yan JH (2017) An optical investigation of multiple diesel injections in CNG/diesel dual-fuel combustion in a light duty optical diesel engine. SAE Technical Paper, 2017-01-0755. https://doi.org/10.4271/2017-01-0755

Papagiannakis RG, Hountalas DT, Rakopoulos CD (2007) Theoretical study of the effects of pilot fuel quantity and its injection timing on the performance and emissions of a dual fuel diesel engine. Energy Conversion and Management 48: 2951-2961. https://doi.org/10.1016/j.enconman.2007.07.003

Papagiannakis RG, Krishnan SR, Rakopoulos DC, Srinivasan KK, Rakopoulos CD (2017) A combined experimental and theoretical study of diesel fuel injection timing and gaseous fuel/diesel mass ratio effects on the performance and emissions of natural gas-diesel HPDI engine operating at various loads. Fuel 202: 675-687. https://doi.org/10.1016/j.fuel.2017.05.012

Rahimi A, Fatehifar E, Saray RK (2010) Development of an optimized chemical kinetic mechanism for homogeneous charge compression ignition combustion of a fuel blend of n-heptane and natural gas using a genetic algorithm. Proceedings of the Institution of Mechanical Engineers, Part D: Journal of Automobile Engineering 224: 1141-1159. https://doi.org/10.1243/09544070jauto1343

Sankesh D, Lappas P (2020) An experimental and numerical study of natural gas jets for direct injection internal combustion engines. Fuel 263: 116745. https://doi.org/10.1016/j.fuel.2019.116745

Sankesh D, Petersen P, Lappas P (2018) Flow characteristics of natural-gas from an outward-opening nozzle for direct injection engines. Fuel 218: 188-202. https://doi.org/10.1016/j.fuel.2018.01.009

Thangaraja J, Kannan C (2016) Effect of exhaust gas recirculation on advanced diesel combustion and alternate fuels-a review. Applied Energy 180: 169-184. https://doi.org/10.1016/j.apenergy.2016.07.09

Wang CY, Liu FS, Wu WF (2012) Experimental study of the impinging jet diffusion and entrainment for high-pressure injected methane. Transactions of CSIC 30: 423-428. (in Chinese) https://doi.org/10.16236/j.cnki.nrjxb.2012.05.011

Wang ZS, Zhao ZX, Wang D, Tan MZ, Han YQ, Liu ZC, Dou HL (2016) Impact of pilot diesel ignition mode on combustion and emissions characteristics of a diesel/natural gas dual fuel heavy-duty engine. Fuel 167: 248-256. https://doi.org/10.1016/j.fuel.2015.11.077

Wei LJ, Geng P (2016) A review on natural gas/diesel dual fuel combustion, emissions and performance. Fuel Processing Technology 142: 264-278. https://doi.org/10.1016/j.fuproc.2015.09.018

Wei LJ, Yao CD, Wang QG, Pan W, Han GP (2015) Combustion and emission characteristics of a turbocharged diesel engine using high premixed ratio of methanol and diesel fuel. Fuel 140: 156-163. https://doi.org/10.1016/j.fuel.2014.09.070

Zhang Q, Li MH, Shao SD (2015) Combustion process and emissions of a heavy-duty engine fueled with directly injected natural gas and pilot diesel. Applied Energy 157: 217-228. https://doi.org/10.1016/j.apenergy.2015.08.021

Zhang Z, Liu HF, Yue ZY, Wu YY, Kong XG, Zheng ZQ, Yao MF (2022) Effects of multiple injection strategies on heavy-duty diesel energy distributions and emissions under high peak combustion pressures. Frontiers in Energy Research 10: 857077. https://doi.org/10.3389/fenrg.2022.857077

Zheng ZQ, Yue L, Liu HF, Zhu YX, Zhong XF, Yao MF (2015) Effect of two-stage injection on combustion and emissions under high EGR rate on a diesel engine by fueling blends of diesel/gasoline, diesel/n-butanol, diesel/gasoline/n-butanol and pure diesel. Energy Conversion and Management 90: 1-11. https://doi.org/10.1016/j.enconman.2014.11.011

Zoldak P, Sobiesiak A, Bergin M, Wickman DD (2014) Computational study of reactivity controlled compression ignition (RCCI) combustion in a heavy-duty diesel engine using natural gas. SAE Technical Paper 1: 2014-01-1321. https://doi.org/10.4271/2014-01-1321

Zoldak P, Sobiesiak A, Wickman D, Bergin M (2015) Combustion simulation of dual fuel CNG engine using direct injection of natural gas and diesel. SAE Technical Paper 8(2): 2015-01-0851. https://doi.org/10.4271/2015-01-0851